Available online at www.sciencedirect.com

ScienceDirect

IFAC PapersOnline CONFERENCE PAPER ARCHIVE

IFAC PapersOnLine 55-16 (2022) 196–201

Artificial pancreas under periodic MPC for trajectory tracking: handling circadian variability of insulin sensitivity

Pablo Abuin * **Antonio Ferramosca** ** **Chiara Toffanin** ***
Lalo Magni **** **Alejandro H. Gonzalez** *

* *Institute of Technological Development for the Chemical Industry (INTEC), CONICET-Universidad Nacional del Litoral (UNL), Santa Fe, Argentina. Email: pabloabu.g@gmail.com*
** *Department of Management, Information and Production Engineering, University of Bergamo, Bergamo Italy*
*** *Department of Electrical, Computer and Biomedical Engineering, University of Pavia, Pavia, Italy*
**** *Department of Civil and Architecture Engineering, University of Pavia, Pavia, Italy*

Abstract: Closed-loop glycemic control algorithms have demonstrated the ability to improve glucose regulation in patients with type 1 diabetes mellitus (T1D), both in silico and clinical trials. Many of the proposed control strategies have been developed, based on time-invariant linear models, without considering the parametric variations of T1DM subjects. In this work, a pulsatile Zone Model Predictive Control (pZMPC) is proposed, which explicitly considers patterns of intra-day insulin sensitivity (S_I), according to the latest updates of the FDA-approved UVA/Padova simulator. Results show a significant improvement in the performance, which *a-priori* justifies the increment in the controller complexity.

Keywords: Insulin sensitivity variations, trajectory tracking, MPC, Artificial Pancreas

1. INTRODUCTION

Blood glucose regulation in type 1 diabetes (T1D) patients is not an easy task: glucose metabolism is affected by several factors during the day, such as daily variations in subject physiological parameters, different composition of ingested meals, physical activity, irregular pattern of sleep, stress, illness, menstrual cycle, etc (Kudva et al., 2014; Mansell et al., 2017). Among them, circadian variability (24-h) of insulin sensitivity (S_I) is a well known phenomenon that occurs in T1D subjects, characterized by a periodic insulin sensitivity pattern, being lower, on average, at breakfast in comparison with lunch and dinner (Hinshaw et al., 2013). Although this pattern has been associated with the effect of counter-regulatory hormones (i.e. cortisol, melatonin, growth hormone) (Schrezenmeir et al., 1993) or the so-called dawn phenomena, a study conducted by (Hinshaw et al., 2013) did not find such a link, arguing that the modulation of diurnal patterns of S_I could be more related to sleep architecture. Moreover, in comparison with healthy S_I pattern, they noted a large inter-subject variability in T1D patients, which was later corroborated by (Visentin et al., 2015) who, using a minimal model for S_I estimation, detected 7 classes of S_I profiles.

Several mathematical models of the S_I profile have been proposed employing piecewise, sinusoidal and variable basis (Mansell et al., 2017). Indeed, this effect has been included in the UVA/Padova Maximal Model (Visentin et al., 2018) by modifying parameters, such as k_{p3} and V_{mx}, according to a given S_I class. In addition, some control algorithms have been formulated considering intra-patient variability, but few of them have explicitly taken into account the periodicity of the S_I patterns due to circadian variability, to make predictions. Recently, some new adaptive strategies were also proposed. By taking into account that the meal intake and physical activity follow a periodicity pattern, (Ortmann et al., 2017) has proposed a Gaussian-process controller with an offset free Model Predictive Controller (MPC) approach to make predictions under the mini-pig model. Moreover, (Toffanin et al., 2013) used the circadian S_I variability to formulate a dynamic Insulin-on-Board (IOB) constraint for the MPC controller previously presented in (Patek et al., 2012). Finally, (Gondhalekar et al., 2016) proposed to include a periodic reference in order to tackle S_I circadian variability, avoiding overnight hypoglycemia.

In this work, we explicitly consider S_I intra-day variability in the prediction model, which leads to the concept of basal trajectories - in contrast to basal fixed levels. Basal trajectories increase the general system controllability, to better avoid hypo and hyperglycemia episodes. On the one hand, when the S_I is high, a reasonable option is to keep the glycemia in a high basal level, to counteract eventual falls due to miss-estimation of the S_I. On the other hand, when the S_I is low, a reasonable option is to keep the glycemia in a low basal level, to prevent the insufficient effect of insulin boluses that compensate meals. Further benefits of MPC that are exploited in this work are: the consideration of 'zones objectives' around the basal glycemic trajectories, which define the normoglycemia range and avoid over control (Gondhalekar et al., 2016, 2018; Abuin et al., 2020); asymmetric cost functions (penalizing harder hypoglycemic than hyperglycemic episodes) (Gondhalekar et al., 2016; Abuin et al., 2020); and the use of pulsatile insulin infusions (González et al., 2020; Abuin et al., 2020), which better

10.1016/j.ifacol.2022.09.023

reproduces the pump behavior both, in basal and postprandial scenarios.

Notation: $\mathbb{R}$ and $\mathbb{I}$ are the sets of real and integer numbers. $\mathbb{R}^n_{[a,b]}$ ($\mathbb{R}^n_{(a,b)}$) is the set of real vectors x, of dimension n, which component-wise fulfill $a \leq x \leq b$ ($a < x < b$). Similarly, $\mathbb{I}_{[a,b]}$ ($\mathbb{I}_{(a,b)}$) is the set of integers k such that $a \leq k \leq b$ ($a < k < b$). The n-norm for vectors $x \in \mathbb{R}^n$, with $n \in \mathbb{I}_{[1,\infty)}$, is denoted $\|x\|_n$. Given a set $\mathcal{X} \subseteq \mathbb{R}^n$, $\mathcal{P}(\mathcal{X})$ is the power set of $\mathcal{X}$ (i.e., the set of all subsets of $\mathcal{X}$). $x(\cdot) : \mathbb{R}_{[a,b]} \to \mathbb{R}^n_{[c,d]}$ denotes the continuous-time functions, that goes from $t \in [a,b]$ to real vectors in $\mathbb{R}^n_{[c,d]}$. Similarly, $\mathbf{x} : \mathbb{I}_{[a,b]} \to \mathbb{R}^n_{[c,d]}$ represents the discrete-time sequences, that goes from $k \in [a,b]$ to vectors in $\mathbb{R}^n_{[c,d]}$.

2. PHYSIOLOGICAL BLOOD GLUCOSE-INSULIN MODEL

The following affine continuous-time time-varying state space model, which is a physiological minimal model based on (Ruan et al., 2016), is considered to describe the **glucose-insulin subsystem** under intra-day variations of insulin sensitivity ($S_I(t)$):

$$\dot{x}(t) = A_x(t)x(t) + B_u u(t) + B_z z(t) + E, \;\; x(0) = x_0, \quad (1)$$

where $x(t) = [x_1(t) \;\; x_2(t) \;\; x_3(t)]'$ denotes the system state, with $x_1 = G$ being the blood glucose concentration [mg/dL], x_2 being the insulin delivery rate in plasma [U/min] and x_3 being the insulin delivery rate in the subcutaneous compartment [U/min], and $u(t)$ denotes the exogenous insulin infusion rate [U/min]. Variable z is a state representing the **meal absorption subsystem**, which is in turn described by the following subsystem:

$$\dot{z}(t) = A_z z(t) + B_r r(t), \;\; z(0) = z_0, \quad (2)$$

where $z(t) = [z_1(t) \;\; z_2(t)]'$, with z_1 being the rate of carbohydrate absorption from the gut [g/min] and z_2 being the glucose delivery rate from the stomach [g/min], and $r(t)$ is the rate of carbohydrate (CHO) intake [g/min].
The subsystems matrices are given by:

$$A_x(t) = \begin{bmatrix} -\theta_1 & -\theta_2(t) & 0 \\ 0 & -\frac{1}{\theta_4} & \frac{1}{\theta_4} \\ 0 & 0 & -\frac{1}{\theta_4} \end{bmatrix}, \; B_u = \begin{bmatrix} 0 \\ 0 \\ \frac{1}{\theta_4} \end{bmatrix}, \; E = \begin{bmatrix} \theta_0 \\ 0 \\ 0 \end{bmatrix},$$
$$B_z = \begin{bmatrix} \theta_3 & 0 \\ 0 & 0 \\ 0 & 0 \end{bmatrix}, \; A_z = \begin{bmatrix} -\frac{1}{\theta_5} & \frac{1}{\theta_5} \\ 0 & -\frac{1}{\theta_5} \end{bmatrix}, \; B_r = \begin{bmatrix} 0 \\ \frac{1}{\theta_5} \end{bmatrix}, \quad (3)$$

where $\theta_2(\cdot) : \mathbb{R}_{[0,\infty)} \to \mathbb{R}_{[\theta_{2min}, \theta_{2max}]}$ is the insulin sensitivity under intra-day variations [mg/(dL·U)] , θ_3 is the raise factor [mg/(dL·g)] and θ_1 is the glucose effectiveness [/min] or glucose self-regulation effect to promote its own metabolism. Furthermore, θ_0 is the extrapolated endogenous glucose production (EGP) at zero glucose and insulin levels [mg/(dL·min)], θ_4 is the insulin absorption kinetics time constant [min], and θ_5 is the meal absorption subsystem time constant [min].
The outputs of subsystem (1) are given by $G(t) = C_1 x(t)$, where $C_1 = [1\ 0\ 0]$ (glycemia to be controlled), and $IOB(t) = C_2 x(t)$ where $C_2 = [0 \;\; \theta_4 \;\; \theta_4]$ (insulin on board, to be constrained for safety reasons).

Assumption 1. *Parameter $\theta_2(\cdot) : \mathbb{R}_{[0,\infty)} \to \mathbb{R}_{[\theta_{2min}, \theta_{2max}]}$ is assumed be $\theta_2(t) := \bar{\theta}_2 + \tilde{\theta}_2(t)$, $t \geq 0$, where $\bar{\theta}_2 > 0$ is a constant nominal value, and $\tilde{\theta}_2(t)$ is a periodic one, accounting for the insulin sensitivity variations due to circadian rhythms: i.e., $\tilde{\theta}_2(t) = \tilde{\theta}_2(t+T)$, for all $t \geq 0$, being T the circadian cycle equal to 24 hours (or 1440 minutes). Furthermore, $\theta_2(t) > 0$ for all $t \geq 0$.*

Subsystems (1) and (2), with $\theta_2(t) \equiv \bar{\theta}_2$, are referred to as the **nominal system**. Note that due to the affine term (E), physiological basal conditions are explicitly accounted for in subsystem (1), since null values of u does not produce null values of G, even in fasting periods where $r(t) \equiv 0$ and $z(t) \equiv 0$.

2.1 Constraints under circadian insulin sensitivity variations

The input and states of subsystem (1) are assumed to be constrained to belong to sets $\mathcal{U}$ and $\mathcal{X}$, respectively. Set $\mathcal{U}$, on one hand, accounts for the positivity and the maximal infusion dose of the insulin pump, and it is given by:

$$\mathcal{U} := \mathbb{R}_{[0, u_{max}]}, \quad (4)$$

with $u_{max} = 15$ [U] (*i.e.*: maximum infusion dose of insulin pumps). Given that - for safety reasons - $IOB(t) = \theta_4(x_2(t) + x_3(t))$ should have different maximum values for different periods of the day, and system (1) is time-variant, the state constraints set $\mathcal{X}$ is defined as a time-variant set. The idea is to consider $\mathcal{X}(\cdot) : \mathbb{R}_{[0,\infty)} \to \mathcal{P}(\mathcal{X})$ periodic, with period T; that is $\mathcal{X}(t) = \mathcal{X}(t+T)$, for all $t \geq 0$. More precisely, the state constraint set $\mathcal{X}(t)$ is given by:

$$\mathcal{X}(t) := \{x \in \mathcal{X} \mid x_{min} \leq Cx \leq x_{max}(t)\}, \quad t \geq 0, \quad (5)$$

with $C = [C_1, C_2]'$, $x_{min} = [G_{hypo}, 0]'$, and $x_{max}(t) = [G_{hyper}, IOB_{max}(t)]'$. $G_{hypo} = 60$ [mg/dL], $G_{hyper} = 250$ [mg/dL], and $IOB_{max}(\cdot) := \theta_4(x_{b,2}(\cdot) + x_{b,3}(\cdot)) + CHO(\cdot)/CR$, with CR representing the carbohydrate-to-insulin ratio, that provides the nominal bolus given by the ratio $CHO(\cdot)/CR$. Moreover, $(x_{b,2}, x_{b,3})$ represent the value of states (x_2, x_3) at a basal trajectory, which will be defined later on.

2.2 Basal conditions analysis

Subsystems (1) and (2) without meal intakes ($r(t) \equiv 0$ and $z(t) \equiv 0$) are referred to as the 'system under basal conditions' and, in such fasting scenario, subsystem (1) describes the whole system dynamic.

Nominal case. For the nominal case (i.e. $\theta_2(t) \equiv \bar{\theta}_2$), the equilibrium set of subsystem (1) is given by a set of pairs (u_s, x_s) fulfilling the condition $x_s = [x_{s,1}, x_{s,2}, x_{s,3}]' = [\frac{\theta_0 - \bar{\theta}_2 u_s}{\theta_1}, u_s, u_s]'$. If, in addition, the input and state constraints are considered, the state equilibrium set is defined as the set of all state x_s that belongs to $\mathcal{X}$, for which there exists some u_s belonging to $\mathcal{U}$. We denote this latter set $\mathcal{X}_s$ and the corresponding input set, $\mathcal{U}_s$.
Among the pairs $(x_s, u_s) \in \mathcal{X}_s \times \mathcal{U}_s$ we define the nominal basal equilibrium (x_b, u_b) as the one corresponding to a specific value of $x_{s,1} := \bar{G}_b$, where $\bar{G}_b$ represents a fixed **basal level for the glucose** (usually $\bar{G}_b = 110$ [mg/dL]). This way, we have a basal equilibrium state $x_b = [\bar{G}_b, u_b, u_b]'$, and a basal equilibrium input $u_b = \frac{\theta_0 - \theta_1 \bar{G}_b}{\bar{\theta}_2}$. See Figure 1 for a schematic plot of $\mathcal{X}_s$ (blue line) and x_b (green point).

Time-varying case. If now $\theta_2(t) = \bar{\theta}_2 + \tilde{\theta}_2(t)$, with a periodic $\theta_2(t) = \theta_2(t+T)$, for $t \geq 0$, **the whole concept of equilibrium is lost**, i.e., there is no longer an input that maintains the state fixed in time. However, as long as $\theta_2(t)$ is not large enough to cause feasibility problems, it is still possible to define a trajectory such that $G(t) = x_1(t)$ remains

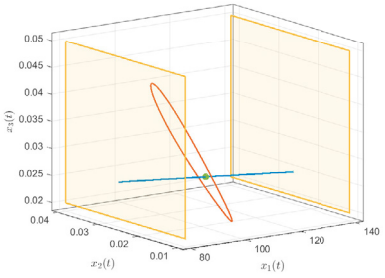

Fig. 1. Equilibrium set $\mathcal{X}_s$ (blue line), basal state x_b (green point) and basal trajectory corresponding to $\bar{G}_b = 110$ (red periodic trajectory), for subsystem (1). The yellow planes represents bounds for $G = x_1$

fixed at $\bar{G}_b$, while the other two states $x_2(t)$ and $x_3(t)$ are periodic as it is $\theta_2(t)$. This trajectory of period T, defined as $x_b(t) := [x_{b,1}(t), x_{b,2}(t), x_{b,3}(t)]' = [\bar{G}_b, x_{b,2}(t), x_{b,3}(t)]'$, $t \geq 0$, corresponds to a periodic input $u_b(t)$, and can be obtained explicitly as follows:

$$x_b(t) = \begin{bmatrix} x_{b,1}(t) \\ x_{b,2}(t) \\ x_{b,3}(t) \end{bmatrix} = \begin{bmatrix} \bar{G}_b \\ \frac{\theta_0 - \bar{G}_b\theta_1}{\theta_2(t)} \\ \frac{\theta_0 - \bar{G}_b\theta_1}{\theta_2(t)} - \frac{(\theta_0 - \bar{G}_b\theta_1)\theta_4\dot{\theta}_2(t)}{\theta_2^2(t)} \end{bmatrix}, \quad (6)$$

with $u_b(t) = x_{b,3}(t) + \theta_4\dot{x}_{b,3}(t)$. Figure 1 shows a schematic plot of $x_b(t)$ (red trajectory).

The latter periodic trajectory $x_b(t)$ is, however, one of many possible (the one that maintains $x_1(t)$ at $\bar{G}_b$). In a more general framework, we may propose a problem to find out the basal state and input trajectories, such that state $x_1(t)$ approaches as long as possible (i.e., fulfilling the constraints) a general G_b^{ref}, periodic in $[0, T]$. The following definition summarizes this new concept:

Definition 1 (Basal state and input trajectories)**.** *Consider subsystem* (1) *constrained by $\mathcal{X}$ and $\mathcal{U}$, and a given glycemia periodic reference $G_b^{ref}(\cdot) : \mathbb{R}_{[0,\infty)} \to \mathbb{R}_{[G_{hypo}, G_{hyper}]}$, with period T (i.e., $G_b^{ref}(t) = G_b^{ref}(t+T)$, for $t \geq 0$). A basal state and input trajectories are given by the periodic state trajectory $x_b(\cdot) : \mathbb{R}_{[0,\infty)} \to \mathcal{X}$ and the corresponding input $u_b(\cdot) : \mathbb{R}_{[0,\infty)} \to \mathcal{U}$ that minimizes $\|C_1 x_b(t) - G_b^{ref}(t)\|$, for $t \geq 0$.*

Remark 1. *Note that the concept of basal state and input trajectories can be also defined for LTI models. However, the periodic (and significant) variability of S_I (which is not considered in LTI models) may reinforce low values of G, so producing hypoglycemic episodes.*

3. IDENTIFICATION OF CIRCADIAN S_I RHYTHMS

In order to obtain an estimation of the periodic insulin sensitivity pattern, $\theta_2(t)$, a constrained optimization problem was formulated by imposing a periodicity constraint on the time-varying parameter. Furthermore, physiological constraints were added for $\theta_2(t)$ estimation, such that $\theta_2(t) \in \Theta$, with $\Theta = \mathbb{R}_{[0.8\alpha\bar{\theta}_2, 1.2\bar{\theta}_2]}$ ($\alpha = 0.4$) and $\bar{\theta}_2$ being the insulin sensitivity nominal value. A variability of $\pm 20\%$ was assumed, as reported in (Visentin et al., 2015). The system period was fixed in a daily basis ($T = 1440$ min) so the circadian insulin sensitivity rhythm can be computed as the solution of the following constrained convex quadratic problem:

$$\begin{aligned} \theta_2^* = \arg\min_{\theta_2, \theta_{2T}, \mathbf{s}} \; & \textstyle\sum_{j=1}^{N_{CI}} \|G_m(j) - G(j)\|_2^2 + \lambda_1 \|s(j)\|_2^2 \\ & + \lambda_2 \|\Delta\theta_{2T}(j)\|_1 \\ s.t. \; & G(j) = C_1[\tfrac{(q-1)I}{T_s} - A_x(j)]^{-1}(B_u u(j) \\ & + B_z z(j) + E), \quad j \in \mathbb{I}_{[0,N_{CI}]}, \\ & z(j) = [\tfrac{(q-1)I}{T_s} - A_z]^{-1} B_r r(j), \; j \in \mathbb{I}_{[0,N_{CI}]}, \\ & \theta_2(j) \leq \theta_{2T}(j) + s(j), \quad j \in \mathbb{I}_{[0,N_{CI}]}, \\ & \theta_2(j) \geq \theta_{2T}(j) - s(j), \quad j \in \mathbb{I}_{[0,N_{CI}]}, \\ & \theta_{2T}(j) = \theta_{2T}(j+T), \theta_2(j) \in \Theta, \; j \in \mathbb{I}_{[0,N_{CI}]} \\ & s(j) \geq 0, \quad j \in \mathbb{I}_{[0,N_{CI}]}, \end{aligned}$$

where θ_2^* is the optimal estimation of the daily circadian S_I pattern, $\lambda_1, \lambda_2 > 0$ are penalty scalars, $G_m(j)$ denotes the measured BG, $G(j)$ is the BG predicted by the model, q is a forward shift operator ($qx(j) := x(j+1)$), θ_{2T} is an auxiliary periodic variable, and s a dispersion/slack variable. $A_x(j)$ indicates that the state space matrix varies throughout the prediction horizon, due to the time variability of $\theta_2(j)$ (Euler discretization). N_{CI} is the length of the dataset ($N_{days} \cdot (288/day)$, if $T_s = 5$ min). Due to the inherent inter-day variability of the insulin sensitivity, $\theta_2(t) \approx \theta_2(t+T)$ (quasi-periodic behavior), so the periodic constraint was relaxed via the slack variable $s(j)$, whose variations are penalized by the l-2 norm regularization term (weighted by $\lambda_1 \geq 0$). In addition, since the S_I profile follows a piecewise constant evolution, a sparsity-promotion term of the first order time differences, given by $\Delta\theta_{2T}(j) = \theta_{2T}(j) - \theta_{2T}(j-1)$, was included in order to detect S_I transitions over periods of flat S_I progression.

4. DISCRETE-TIME LTV MODELING FOR PULSIVE INPUT SIGNALS

In order to use the continuous-time models (1) and (2) as prediction models in an MPC controller, they should be previously sampled. We select in this work the pulsatile scheme proposed in (Abuin et al., 2020) which, for a given sampling time T_s (such that T is a multiple of T_s) and a pulse duration $0 < \Delta < T_s$, consists in the following discrete-time submodels:

$$\begin{aligned} x(k+1) &= F_x(k, x(k), u(k), z(k)), \\ z(k+1) &= F_z(z(k), r(k)), \\ G(k) &= C_1 x(k), \quad IOB(k) = C_2 x(k), \end{aligned} \quad (7)$$

where $k \in \mathbb{I}_{[0,\infty)}$ represents kT_s, $F_x(\cdot, x(\cdot), u(\cdot), z(\cdot)) := A_x^d(\cdot)x(\cdot) + B_u^d(\cdot)u(\cdot) + B_z^d(\cdot)z(\cdot) + E^d(\cdot)$ and $F_z(z(\cdot), r(\cdot)) := A_z^d z(\cdot) + B_r^d r(\cdot)$. The time varying pulsatile discrete-time matrices are: $A_x^d(k) := e^{A_x(kT_s)T_s}$, $B_u^d(k) := e^{A_x(kT_s)(T_s - \Delta T_s)} A_x^{-1}(kT_s)(e^{A_x(kT_s)\Delta T_s} - I_3)B_u$, $B_z^d(k) := A_x^{-1}(kT_s)(e^{A(kT_s)T_s} - I_3)B_z$, $E^d(k) := A_x^{-1}(kT_s)(e^{A_x(kT_s)T_s} - I_3)E$, $A_z^d := e^{A_z T_s}$, and $B_r^d := A_z^{-1}(e^{A_z T_s} - I_2)B_r$ (Abuin et al., 2020).

Note that in the previous discretization it was assumed that $\theta_1 \neq 0$ (in such a way that A_x is invertible) and time varying parameters are assumed constant during the sampling-time interval T_s, that is, $\theta_2(t) := \theta_2(kT_s)$, $t \in [kT_s, (k+1)T_s)$, $k \in \mathbb{I}_{[0,\infty)}$ (zero-order hold assumption). Furthermore, the time-varying state constraints set, $\mathcal{X}(t)$, can be sampled by considering $\mathcal{X}(k) := \mathcal{X}(kT_s)$, $k \in \mathbb{I}_{[0,\infty)}$.

5. PULSATILE MPC FORMULATIONS

In this section, a pulsatile MPC controller devoted to track the **basal state and input trajectories** is presented, which is based on concepts introduced in (Limon et al., 2015) and (Abuin et al., 2020). Although the MPC is designed for both, the announced

(or partially-announced) and the unannounced meal cases, in the present work only the (not in advanced) announced meal case will be considered. The general control problem can be defined as follows:

Definition 2 (Control problem: basal trajectory tracking)**.** *Consider system* (7) *constrained by* $\mathcal{X}(k)$, $k \in \mathbb{I}_{[0,\infty)}$ *and* $\mathcal{U}$, *and a desired basal reference for the blood glucose* $\mathbf{G}_b^{ref} : \mathbb{I}_{[0,\infty)} \to \mathbb{R}_{[G_{hypo},G_{hyper}]}$, *with period* T, *which is a sampled version of* $G_b^{ref}(\cdot)$, *in Definition 1, and* T *is now the period in sampling times. Then, given the estimated states* $\hat{x}$ *and* $\hat{z}$ *and the meal announcement* $\hat{r}$, *at the current time* k, *the control problem consists in steering the system to the basal state and input trajectory* [1], *denoted as* $\mathbf{x}_b(\cdot) : \mathbb{I}_{[0,\infty)} \to \mathcal{X}$ *and* $\mathbf{u}_b(\cdot) : \mathbb{I}_{[0,\infty)} \to \mathcal{U}$, *which minimize* $\|C_1 x_b(k) - G_b^{ref}(k)\|$, *for all* $k \geq 0$.

To account for the latter control problem, the following MPC schemes are proposed.

5.1 Basal trajectory tracking, two stage approach

Given $G_b^{ref}(k)$, over the period $[0, T]$, we solve first the **basal trajectory computation problem**, $\mathcal{BTC}(\mathbf{G}_b^{ref})$, to obtain $\mathbf{u}_b$ and $\mathbf{x}_b$:

$$\begin{aligned} \min_{\bar{\mathbf{u}}_b, \bar{\mathbf{x}}_b} \; & V_{traj}(\mathbf{G}_b^{ref}; \bar{\mathbf{u}}_b, \bar{\mathbf{x}}_b) \\ s.t. \; & \bar{u}_b(j) \in \mathcal{U}, \;\; \bar{x}_b(j) \in \mathcal{X}(k+j), \qquad j \in \mathbb{I}_{[0,T]} \\ & \bar{x}_b(j+1) = F_x(k+j, \bar{x}_b(j), \bar{u}_b(j), 0), \\ & \bar{x}_b(0) = F_x(k+T-1, \bar{x}_b(T-1), \bar{u}_b(T-1), 0), \end{aligned} \tag{8}$$

with $\mathcal{U}$, $\mathcal{X}$ given by (4) - (5), respectively, and V_{traj} given by:

$$V_{traj}(\mathbf{G}_b^{ref}; \bar{\mathbf{u}}_b, \bar{\mathbf{x}}_b) := \sum_{j=0}^{T-1} S \|C_1 \bar{x}_b(j) - G_b^{ref}(j)\|_2^2, \tag{9}$$

with $S > 0$ being an appropriate positive penalty.

The solution of problem $\mathcal{BTC}(\mathbf{G}_b^{ref})$ is given by $\bar{\mathbf{x}}_b^0(\cdot) : \mathbb{I}_{[0,T]} \to \mathcal{X}$ and $\bar{\mathbf{u}}_b^0(\cdot) : \mathbb{I}_{[0,T]} \to \mathcal{U}$, which fulfills $\bar{x}_b^0(0) = \bar{x}_b^0(T)$ and $\bar{u}_b^0(0) = \bar{u}_b^0(T)$, respectively. Note that if $G_b^{ref}(k)$ is reachable over the period $[0, T]$, then $V_{traj}(\mathbf{G}_b^{ref}; \bar{\mathbf{u}}_b^0, \bar{\mathbf{x}}_b^0) = 0$, since in such case, the blood glucose reference can be followed by means of a feasible insulin trajectory, and following a feasible state trajectory, over $[0, T]$. Otherwise, $V_{traj}(\mathbf{G}_b^{ref}; \bar{\mathbf{u}}_b^0, \bar{\mathbf{x}}_b^0) > 0$, but given that the later optimization problem is convex, the solution $\bar{\mathbf{u}}_b^0$ and $\bar{\mathbf{x}}_b^0$ is unique.

Once $\bar{\mathbf{u}}_b^0$ and $\bar{\mathbf{x}}_b^0$ are obtained from $\mathcal{BTC}(\mathbf{G}_b^{ref})$, **the basal state and input trajectories** [2], $\mathbf{u}_b$ and $\mathbf{x}_b$, are obtained by concatenating $\bar{\mathbf{u}}_b^0$ and $\bar{\mathbf{x}}_b^0$ over all the positive discrete times, in such a way that $u_b(k) = u_b(k+T)$ and $x_b(k) = x_b(k+T)$, respectively, for all $k \geq 0$.

Consider now the estimated states [3] $\hat{x}$, $\hat{z}$ and the carb counting, $\hat{r}$, at the current time k. The meal announcement sequence $\mathbf{r} : \mathbb{I}_{[0,T]} \to \mathbb{R}_{[0,r_{max}]}$, is such that $r(k) = \hat{r}$ if $k = 0$, and $r(k) = 0$, otherwise. Then, the MPC **trajectory tracking problem**, $\mathcal{MPC}_{\mathcal{TT}}(\hat{x}, \hat{z}, \mathbf{r}, \mathbf{u}_b, \mathbf{x}_b, k)$, to be solved at each time k, is given by:

$$\begin{aligned} \min_{\mathbf{u}} \; & V_{track}(\hat{x}, \hat{z}, \mathbf{r}, \mathbf{u}_b, \mathbf{x}_b, k; \mathbf{u}) \\ s.t. \; & x(0) = \hat{x}, \;\; z(0) = \hat{z} \\ & x(j+1) = F_x(k+j, x(j), u(j), z(j)), \quad j \in \mathbb{I}_{[0,N]} \\ & z(j+1) = F_z(z(j), r(j)), \qquad\qquad\;\; j \in \mathbb{I}_{[0,N]} \\ & u(j) \in \mathcal{U}, \;\; x(j) \in \mathcal{X}(k+j), \qquad\;\; j \in \mathbb{I}_{[0,N-1]} \\ & x(N) = x_b(N), \end{aligned} \tag{10}$$

where $N<T$ is the control horizon and V_{track} is given by:

$$\begin{aligned} V_{track}(\hat{x}, \hat{z}, \mathbf{r}, \mathbf{u}_b, \mathbf{x}_b, k; \mathbf{u}) := & \sum_{j=0}^{N-1} Q \|x(j) - x_b(k+j))\|_2^2 \\ & + R \|u(j) - u_b(k+j)\|_2^2, \end{aligned} \tag{11}$$

with $Q>0$ and $R>0$ being positive definite penalty matrices. In problem $\mathcal{MPC}_{\mathcal{TT}}(\hat{x}, \hat{z}, \mathbf{r}, \mathbf{u}_b, \mathbf{x}_b, k)$, $\hat{x}$, $\hat{z}$, $\mathbf{u}_b$, $\mathbf{x}_b$, $\mathbf{r}$ are parameters, while $\mathbf{u} : \mathbb{I}_{[0,N]} \to \mathcal{U}$ is the optimization variable. Once problem $\mathcal{MPC}_{\mathcal{TT}}$ is solved, the optimal solution is denoted $\mathbf{u}^0$, with an associated state sequence $\mathbf{x}^0$. Following the receding horizon control (RHC) policy, only the first optimal input/dose, $u^0(0)$, is applied to the patient, time goes from k to $k+1$, and the whole problem $\mathcal{MPC}_{\mathcal{TT}}$ is solved again. It can be shown that the control scheme derived from the application of $\mathcal{MPC}_{\mathcal{TT}}$ - provided that Problem $\mathcal{BTC}$ has a unique solution - steers the system feasibly to $\mathbf{u}_b, \mathbf{x}_b$ as $k \to \infty$.

5.2 Basal trajectory tracking, single stage approach

Now, based on the use of artificial trajectory, originally introduced in (Limon et al., 2015), the core idea is to merge both, $\mathcal{BTC}$ and $\mathcal{MPC}_{\mathcal{TT}}$ problems, in a single one, denoted by $\mathcal{MPC}_{\mathcal{BTT}}$. Given $\hat{x}$, $\hat{z}$, $\hat{r}$ and $\mathbf{G}_b^{ref}$, at the current time k, the cost function of the problem to be solved at k is given by:

$$\begin{aligned} V_N(\hat{x}, \hat{z}, \mathbf{r}, \mathbf{G}_b^{ref}, k; \mathbf{u}, \mathbf{u}_a, \mathbf{x}_a) := & V_{track}(\hat{x}, \hat{z}, \mathbf{r}; \mathbf{u}, \mathbf{u}_a, \mathbf{x}_a) \\ & + V_{traj}(\mathbf{G}_b^{ref}, k; \mathbf{u}_a, \mathbf{x}_a) \end{aligned} \tag{12}$$

where

$$\begin{aligned} V_{track}(\hat{x}, \hat{z}, \mathbf{r}; \mathbf{u}, \mathbf{u}_a, \mathbf{x}_a) := & \sum_{j=0}^{N-1} Q \|x(j) - x_a(j))\|_2^2 \\ & + R \|u(j) - u_a(j)\|_2^2, \end{aligned} \tag{13}$$

is a term designed to steer the system to the artificial trajectory variables $\mathbf{u}_a : \mathbb{I}_{[0,T]} \to \mathcal{U}$, $\mathbf{x}_a : \mathbb{I}_{[0,T]} \to \mathcal{X}$, in the transient regime, and

$$V_{traj}(\mathbf{G}_b^{ref}, k; \mathbf{u}_a, \mathbf{x}_a) := \sum_{j=0}^{T-1} S \|C_1 x_a(j) - G_b^{ref}(k+j)\|_2^2 \tag{14}$$

is a term devoted to steer the state artificial trajectory to the desired basal reference $\mathbf{G}_b^{ref}$.

The optimization problem $\mathcal{MPC}_{\mathcal{BTT}}(\hat{x}, \hat{z}, \mathbf{r}, \mathbf{G}_b^{ref}, k)$ to be solved by the MPC is then given by:

$$\begin{aligned} \min_{\mathbf{u}, \mathbf{u}_a, \mathbf{x}_a} \; & V_N(\hat{x}, \hat{z}, \mathbf{r}, \mathbf{G}_b^{ref}, k; \mathbf{u}, \mathbf{u}_a, \mathbf{x}_a) \\ s.t. \; & x(0) = \hat{x}, \;\; z(0) = \hat{z} \\ & x(j+1) = F_x(k+j, x(j), u(j), z(j)), \quad j \in \mathbb{I}_{[0,N]} \\ & z(j+1) = F_z(z(j), r(j)), \qquad\qquad\;\; j \in \mathbb{I}_{[0,N]} \\ & u(j) \in \mathcal{U}, \;\; x(j) \in \mathcal{X}(k+j), \qquad\;\; j \in \mathbb{I}_{[0,N-1]} \\ & x(N) = x_a(N), \\ & x_a(j+1) = F_x(k+j, x_a(j), u_a(j), 0), \;\; j \in \mathbb{I}_{[0,T-1]} \\ & u_a(j) \in \mathcal{U}, \quad x_a(j) \in \mathcal{X}(k+j), \qquad j \in \mathbb{I}_{[0,T-1]} \\ & x_a(0) = F_x(k+T-1, x_a(T-1), u_a(T-1), 0). \end{aligned} \tag{15}$$

Notice that this approach is convenient (i) to allow changes in $\mathbf{G}_b^{ref}$ profile, that are instantaneously accounted for in the single optimization problem (i.e., terminal constraint does not

[1] That can be seen as a sampled version of $x_b(\cdot)$ and $u_b(\cdot)$, of Definition 1

[2] Note that $\bar{\mathbf{u}}_b^0$ and $\bar{\mathbf{x}}_b^0$ are defined over $[0, T]$ while the basal state and input trajectories, $\mathbf{x}_b$ and $\mathbf{u}_b$, are defined over $[0, \infty)$

[3] The states x and z are assumed to be estimated by an output disturbance observer (ODO) as the one presented in Abuin et al. (2020)

depend on a pre-computed basal trajectory), and (ii) to enlarge the domain of attraction of the controller (i.e., due to the fact of having a basal reachable trajectory as a decision variable instead of a particular one).

5.3 Basal tube tracking

The idea now is to extend the latter formulation to the case of zone control, that is, control schemes in which the control objective is to follow a region or zone of possible values of G (or a tube made of several zones varying over the time) instead of a particular reference. Taking advantage of the use of artificial variables, this extension can be made by replacing the trajectory cost (14), V_{traj}, by

$$V_{traj}(\mathbf{G}_b^{ref}, k; \mathbf{u}_a, \mathbf{x}_a, \mathbf{G}*) := \sum_{j=0}^{T-1} S\|C_1 x_a(j) - G^*(j)\|_2^2,$$

where $G^*(j)$ is an additional optimization variable, only restricted by $G^*(j) \in [G_b^{ref}(k+j) - G_{b,min}^z, G_b^{ref}(k+j) + G_{b,max}^z]$, being $G_{b,min}^z$ and $G_{b,max}^z$ the lower and upper bounds of the zone, respectively. Moreover, following the ideas presented in (Abuin et al., 2020, Section 6), it is possible to consider asymmetric tubes, by harder penalizing the excursion of $G(t)$ under the reference value $\mathbf{G}_b^{ref}$.

For the sake of brevity, we do not analyse here the feasibility and stability of the proposed control schemes. However, they can proved by following similar steps as in (Limon et al., 2015).

6. SIMULATIONS RESULTS

The performance of the proposed MPC formulations is evaluated through the commercially available UVA/Padova simulator (T1DMS2013, Academic Version) with a virtual average adult patient ($CR = 22.48$ [g/U]). Sensitivity insulin variations are added, acting on k_{SI}, according to randomly-noisy smoothed variation of the nominal profile reported in (Visentin et al., 2015, 2018). The identification of $\theta_2(t)$ is done offline following what is presented in Section 3. The controller parameters are $Q = 1$, $R = 1$, and $S = 10^2$ for all the cases.

6.1 Assessment of the $\mathcal{MPC}_{\mathcal{TT}}$ and $\mathcal{MPC}_{\mathcal{BTT}}$ formulations: nominal vs time-varying prediction model

In this first case, we evaluate the MPC formulations, with and without trajectory planning, $\mathcal{MPC}_{\mathcal{TT}}$ and $\mathcal{MPC}_{\mathcal{BTT}}$, respectively, when a nominal and a time-varying prediction model is employed. For both configurations, a prediction horizon $N = 30$ (2.5 hours) was proposed, to highlight the potential strengths of defining the planned reachable basal trajectory as a decision variable instead of a fix trajectory. The blood glucose reference was fixed in a constant value, $G_b^{ref} = 110$ [mg/dL].

Figure 2 shows the glycemia evolution under the $\mathcal{MPC}_{\mathcal{TT}}$ employing a nominal LTI (red) and a LTV (blue) prediction model. It can be seen, that the LTV setting manages the insulin delivery in accordance to the circadian variations of $S_I(t)$. As expected, the insulin delivery is reduced in an anticipatory way when a S_I transition from a low S_I^l to a high S_I^h level is predicted over the control horizon (i.e. IOB reduction from 10:00 to 12:00 hs). Similarly, it is increased when a S_I transition from a high to a low level is forecasted (i.e. IOB increment from 16:00 to 18:00 hs). In addition, the meal related-events are better counteracted by the LTV configuration, increasing, for the same carb content, the bolus amplitude over intervals of reduced S_I (i.e. IOB at 7:00 and 12:00 hs, being $CHO = 80$ g).

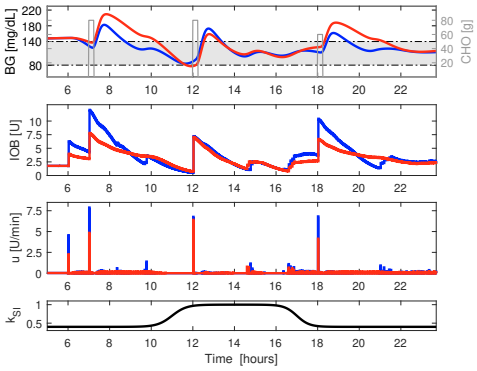

Fig. 2. Blood glucose control employing the $\mathcal{MPC}_{\mathcal{TT}}$ formulation, under nominal LTI (red) and LTV (blue) settings. Insulin sensitivity modulation pattern $k_{SI}(t)$.

Nevertheless, for the $\mathcal{MPC}_{\mathcal{TT}}$ formulation, since its domain of attraction is smaller, a higher number infeasibility episodes are reported (mainly during post prandial intervals, where the BG level is augmented, and thus, feasible control sequences might not be found). See Table 1 for a 7 days scenario.

Table 1. Infeasibility episodes (IE) over 7 days scenario

	$\mathcal{MPC}_{\mathcal{TT}}$		$\mathcal{MPC}_{\mathcal{BTT}}$	
	LTI	LTV	LTI	LTV
#IE	15	52	1	0

6.2 Assessment of the $\mathcal{MPC}_{\mathcal{BTT}}$ formulation: constant vs time-varying G_b^{ref}

In this second case, the idea is to assess the $\mathcal{MPC}_{\mathcal{BTT}}$ performance when a time-varying G_b^{ref} is considered, in such a way that $G_b^{ref}(t) = \lambda(t)G_{b,max}^{ref} + (1-\lambda(t))G_{b,min}^{ref}$, with $\lambda(t) = (\theta_2^{ref}(t) - \theta_{2min}^{ref})/(\theta_{2max}^{ref} - \theta_{2min}^{ref})$. Notice that $\theta_2^{ref}(t) = \max(\theta_2(t) - \overline{\theta_2}, 0)$ to filter eventual non-physiological insulin sensitivity reductions (*i.e.,* $\theta_2(t)$ falling down during postprandial intervals due to structural identifiability limits). To increase the safety from hypoglycemic episodes during intervals of high S_I, the bounds of the time-reference were set in $G_{b,max}^{ref} = 140$ mg/dL and $G_{b,min}^{ref} = 110$ mg/dL. The insulin sensitivity pattern was augmented in 25% (*i.e.,* $k_{SI}^{high}(t) = 1.25 k_{SI}(t)$).

As shown in Figure 3 (i), hypoglycemic episodes are reduced when the aforementioned reference is employed, since it forces the system to steer higher BG levels during periods of high S_I. This strategy allows us to deal with the case in which the identified $\theta_2(t)$ underestimates the actual $S_I(t)$ pattern (*i.e.,* inter-day variability of circadian S_I). Furthermore, if an asymmetric tracking cost is added, the transient evolution before the convergence to the reachable basal trajectory better counteracts the hypoglycemic excursions, thus improving the closed-loop performance. A prediction horizon of $N = 60$ (5 hs) was used in order to increase the influence of the transient regimen effect in the optimization problem $\mathcal{MPC}_{\mathcal{BTT}}$.

6.3 Assessment of the $\mathcal{MPC}_{\mathcal{BTT}}$ (tube): time-varying G_b^{ref}

Finally, in this third case, the $\mathcal{MPC}_{\mathcal{BTT}}$ is compared to $\mathcal{MPC}_{\mathcal{BTT}}$ (tube), where zones are used as control objectives instead of a fixed trajectory. In order to highlight the potential advantages of the latter proposal, a disturbance on the expected circadian variation of $S_I(t)$, given by a physical exercise

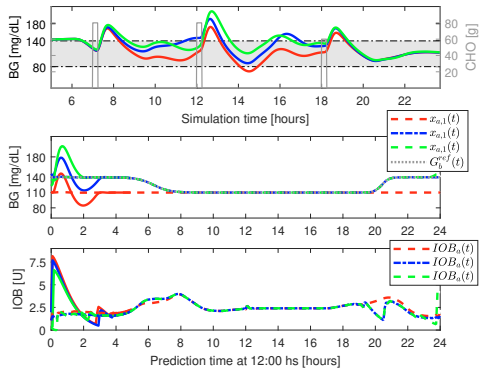

Fig. 3. Blood glucose control using the $\mathcal{MPC}_{\mathcal{BTT}}$ formulation, under: (i) $G_b^{ref} = 110$ mg/dL (red), (ii) $G_b^{ref}(t)$ (blue), and (iii) $G_b^{ref}(t)$ and asymmetric stage cost, $\check{Q}/\hat{Q} = 5 \cdot 10^2$, (green).

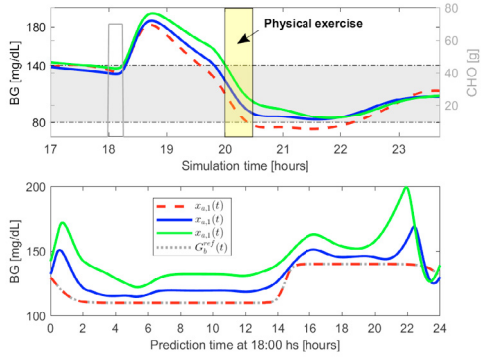

Fig. 4. Blood glucose profile when the control objective is to follow a zone of basal periodic trajectories. $\mathcal{MPC}_{\mathcal{BTT}}$: (red dash-dot line). $\mathcal{MPC}_{\mathcal{BTT}}$ (tube): $G^z_{b,max} = 30$ (blue filled line). $\mathcal{MPC}_{\mathcal{BTT}}$ (wider tube): $G^z_{b,max} = 60$ (green filled line). $G^z_{b,min} = 10$.

episode (moderate exercise 30 min, model C (Dalla Man et al., 2009)) at 20:00 hs was simulated. For both configurations, the time-varying reference proposed in Section 6.2 was considered.

Figure 4 (i) shows that when zones of wider amplitude are employed, the hypoglycemic risk after meal ingestion is reduced. Notice that the periodic basal trajectories (Figure 4 (ii)) are now free to move over a wider zone. The asymmetric cost allows the controller to better anticipate hypoglycemic episodes.

7. CONCLUSION

In this work, a novel trajectory tracking MPC controller that accounts for circadian variability is proposed for the artificial pancreas problem. Although the formulation is (slightly) more complex than classical MPCs, the performance of the simulation on the average virtual patient case-study (in both, the handling of hyper and hypoglycemic episodes) suggests that the strategy may be a first step in a new form of tackling the AP problem under MPC.

REFERENCES

Abuin, P., Rivadeneira, P., Ferramosca, A., and González, A. (2020). Artificial pancreas under stable pulsatile mpc: Improving the closed-loop performance. *Journal of Process Control*, 92, 246–260.

Dalla Man, C., Breton, M.D., and Cobelli, C. (2009). Physical activity into the meal glucose—insulin model of type 1 diabetes: In silico studies.

Gondhalekar, R., Dassau, E., and Doyle III, F.J. (2018). Velocity-weighting and velocity-penalty MPC of an artificial pancreas: Improved safety and performance. *Automatica*, 91(48), 105–117.

Gondhalekar, R., Dassau, E., and Doyle III, F.J. (2016). Periodic zone-mpc with asymmetric costs for outpatient-ready safety of an artificial pancreas to treat type 1 diabetes. *Automatica*, 71, 237–246.

González, A.H., Rivadeneira, P.S., Ferramosca, A., Magdelaine, N., and Moog, C.H. (2020). Stable impulsive zone model predictive control for type 1 diabetic patients based on a long-term model. *Optimal Control Applications and Methods*, 41(6), 2115–2136.

Hinshaw, L., Dalla Man, C., Nandy, D.K., et al. (2013). Diurnal pattern of insulin action in type 1 diabetes: implications for a closed-loop system. *Diabetes*, 62(7), 2223–2229.

Kudva, Y.C., Carter, R.E., Cobelli, C., Basu, R., and Basu, A. (2014). Closed-loop artificial pancreas systems: physiological input to enhance next-generation devices. *Diabetes care*, 37(5), 1184–1190.

Limon, D., Pereira, M., de la Pena, D.M., Alamo, T., Jones, C.N., and Zeilinger, M.N. (2015). Mpc for tracking periodic references. *IEEE Transactions on Automatic Control*, 61(4), 1123–1128.

Mansell, E.J., Docherty, P.D., and Chase, J.G. (2017). Shedding light on grey noise in diabetes modelling. *Biomedical Signal Processing and Control*, 31, 16–30.

Ortmann, L., Shi, D., Dassau, E., Doyle, F.J., Leonhardt, S., and Misgeld, B.J. (2017). Gaussian process-based model predictive control of blood glucose for patients with type 1 diabetes mellitus. In *2017 11th Asian Control Conference (ASCC)*, 1092–1097. IEEE.

Patek, S.D., Magni, L., Dassau, E., Karvetski, C., Toffanin, C., De Nicolao, G., Del Favero, S., Breton, M., Dalla Man, C., Renard, E., et al. (2012). Modular closed-loop control of diabetes. *IEEE Transactions on Biomedical Engineering*, 59(11), 2986–2999.

Ruan, Y., Wilinska, M.E., Thabit, H., and Hovorka, R. (2016). Modeling day-to-day variability of glucose–insulin regulation over 12-week home use of closed-loop insulin delivery. *IEEE Transactions on Biomedical Engineering*, 64(6), 1412–1419.

Schrezenmeir, J., Tatò, F., Tatò, S., Laue, C., and Beyer, J. (1993). Differences between basal and postprandial circadian variation of insulin sensitivity in healthy subjects and type 1 diabetics. In *Hormones in Lipoprotein Metabolism*, 45–64. Springer.

Toffanin, C., Zisser, H., Doyle III, F.J., and Dassau, E. (2013). Dynamic insulin on board: incorporation of circadian insulin sensitivity variation. *Journal of diabetes science and technology*, 7(4), 928–940.

Visentin, R., Campos-Náñez, E., Schiavon, M., Lv, D., Vettoretti, M., Breton, M., Kovatchev, B.P., Dalla Man, C., and Cobelli, C. (2018). The uva/padova type 1 diabetes simulator goes from single meal to single day. *Journal of diabetes science and technology*, 12(2), 273–281.

Visentin, R., Dalla Man, C., Kudva, Y.C., Basu, A., and Cobelli, C. (2015). Circadian variability of insulin sensitivity: physiological input for in silico artificial pancreas. *Diabetes technology & therapeutics*, 17(1), 1–7.